Proceedings of the 7th International Conference on Applied Informatics
Eger, Hungary, January 28–31, 2007. Vol. 1. pp. 175–184.

An empirical method for determining the number of iterations needed in the pre-processing of X-ray images of welds using PCNN algorithms

Coulibaly Sékou Tidiani

College of Kecskemét, GAMF Faculty, Institute of Informatics,
e-mail: sekou.tidiani@gamf.kefo.hu

Abstract

The paper proposes a system of pre-processing for X-ray images of welds that look like textures by mean of Pulse-Coupled Neural Networks (PCNN). In fact the original PCNN and none of its derivative models do not specify any stopping criterion. As the anomalies found in the images show a lot of irregular textels, the paper makes use of co-occurrence matrix based parameters to determine the amount of iterations needed in the PCNN algorithm extended by an iteration counter. The paper first adaptively specifies a co-occurrence matrix among of the possible ones and computes its parameters. In the second stage, these parameters are mapped to PCNN iteration numbers by mean of classical neural network trained for this purpose. The proposed pre-processing produces more deterministic results that embed discriminatory and generalisation properties in the feature vectors. The extended PCNN also produces a geometrical invariant feature sets compared to known classical pre-processing approaches.

Keywords: Texture analysis, PCNN, ANN

1. Introduction

This paper discusses the filtering of industrial welds for their future inspection in computer vision systems. Figure 1 shows X-ray images of welds labelled according to some typical problems of common interest. They images have in common the following properties:

They are not classical patterns having forms or other geometrical features. They are strongly irregular textures and are very noisy. Textels are textural elements that replicate their self over a region of an image with some possible variation in their size, orientation, spread or even the intensity of the pixels composing them.

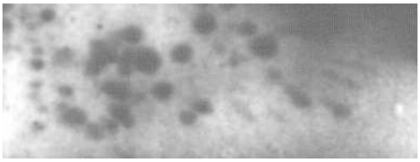

Solid inclusions

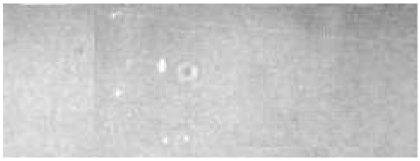

Gas inclusions

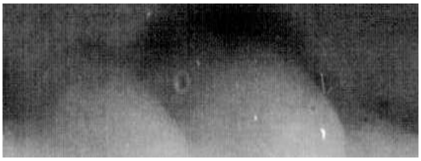

Under-built seam head

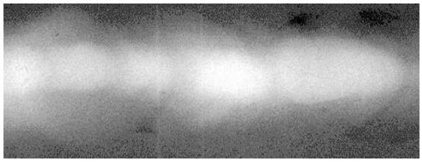

Melt edge

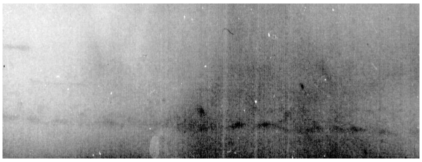

Under-built seam root

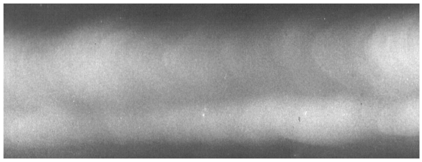

Under-built seam head

Figure 1

Classically, the goal of texture analysis is to quantify properties such as smoothness, coarseness or the regularity. Here the structural approaches are to be discarded because they are suited strictly for ordered textures. The only use of spectral or statistical methods does not lead to a result which meets the goal of enhancing class separation and generalization for further processing in computer vision systems.

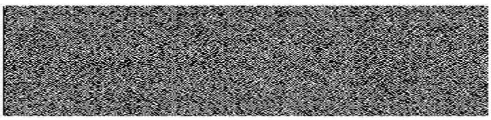

Figure 2

Laws [3] introduced three basic 1x3 spatial filter masks, shown in equation (1.1), $L3$, $E3$ and $S3$ for respectively local averaging, edge detection and spot detection.

$$L3 = [121]; \; E3 = [-101]; \; S3 = [-12-1] \tag{1.1}$$

By convolving pairs of these masks together, other sets of filters can be obtained. It is difficult to filter the weld images by application of classical texture filters without considerable lost of information. Figure 2 shows the degradation caused by some of the filters mentioned above for spots detection.

The lost of information has a serious effect on the discriminative properties of the images and can make difficult or impossible the design of a classifier for them.

This paper takes in consideration recent researches in synergetics of the mammalian visual cortex that have lead to new paradigms in digital image processing. It has been observed that information flows, in form of waves, travels in both directions between the retina and the visual cortex. These patio-temporal entities called auto-waves have been largely studied with the goal to be modelled later. It has been proved that auto-waves essentially differ from classical waves in the following properties: there is no reflection from noises (irregularities) and when two auto-waves collide they are both destructed. These properties are the base for the invariant, under translation, rotation and scaling, visual pattern processing. PCNN are auto-wave-based artificial neural network models that give new opportunities in digital image processing. A comparative study [1] shows the most 20 important neuro-computational features of biological spiking neurons, each of them can be chosen for building and simulating PCNN of different behaviours.

This paper will briefly show in the following an historically important formalism: the Hodgkin-Huxley [2], and two others: the Eckhorn model, which has plenty of parameters to setup and used in simulations with no major time constraints, finally the ICM (Intersecting cortical Model) which computational efficiency is proved and implemented [2] in real world problem solving.

1.1. Models of the visual cortex

1.1.1. The Hodgkin-Huxley model

This first model, built fifty years ago, lays on the cellular membrane potentials as follows:

$$I = m^3 h G_{Na}(E - E_{Na}) + n^4 G_K(E - E_K) + G_L(E - E_L) \tag{1.2}$$

$$\frac{dm}{dt} = a_m(1 - m) - b_m m \tag{1.3}$$

The above equations express the ionic current I across the cellular membrane in terms of E the total potential of relevant chemical components (sodium, potassium and leakage) within the cellule, their respective individual potential (E_K, E_{Na} and E_L) and conductance (G_K, G_{Na} and G_L). The term m is the probability that the ionic current will open transmission channel trough the cell. This model gives the behaviour of neurons in form of differential equation as an oscillatory process. The quantities a_m and b_m are the rate of a particle for not opening and for opening it, and both are functions of E and the chemical element in action (Na or K). A deeper description is found in [2], with more equations and tens of parameters by setting of which the model can emulate all the neuro-computational properties given in [3].

1.1.2. The PCNN/ICM model: architecture and algorithm

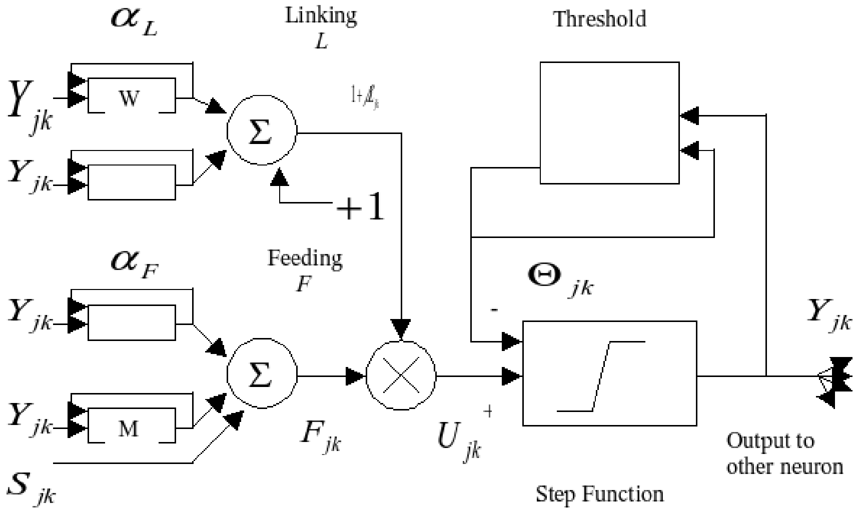

Figure 3

If the Hodgkin-Huxley model is purely behavioural, the PCNN model gives a digital model implementing the Heckhorn's connectionist model, based on studies of the cat visual cortex. Its structure, shown in Figure 3, consists of three parts: the perceptive, the modulation and the output pulse generator. The perceptive part receive stimulus from other neurons through two channels: the feeding F dealing with both a local and an external stimulus, and the linking L, with only the local one. The linking and feeding parts are combined to give U the internal state of the PCNN. The standard PCNN model is computed by evaluating iteratively the following equations:

$$F_{ij}[n] = e^{\alpha F \delta n} F_{ij}[n-1] + S_{ij} + V_F \sum_{kl} M_{ijkl} Y_{kl}[n-1] \tag{1.4}$$

$$U_{ij}[n] = F_{ij}[n]\{1 + \beta L_{ij}[n]\} \tag{1.5}$$

$$L_{ij}[n] = e^{\alpha L \delta n} L_{ij}[n-1] + S_{ij} + V_L \sum_{kl} W_{ijkl} Y_{kl}[n-1] \tag{1.6}$$

$$Y_{ij}[n] = \begin{cases} 1 & if \quad U_{ij}[n] > \Theta_{ij}[n] \\ 0 & \quad Otherwise \end{cases} \tag{1.7}$$

$$\Theta_{ij}[n] = e^{\alpha \Theta \delta n} \Theta_{ij}[n-1] + V_\Theta Y_{ij}[n] \tag{1.8}$$

Where M and W are the synaptic weight-matrices through which the neighbouring neurons communicate with a given PCNN, VF and VL are normalizing constants.

1.1.3. The ICM model

ICM is the simplest and it is the intersection of several visual cortex models [2]. Its internal state F, dynamic threshold Θ_{ij} and output Y are computed as follows:

$$F_{ij}[n+1] = fF_{ij}[n] + S_{ij} + W\{Y\}_{ij} \tag{1.9}$$

$$Y_{ij}[n+1] = \begin{cases} 1 & if \quad F_{ij}[n+1] > \Theta_{ij}[n] \\ 0 & \quad Otherwise \end{cases} \tag{1.10}$$

$$\Theta_{ij}[n+1] = g\Theta_{ij}[n] + hY_{ij}[n+1] \tag{1.11}$$

where f, g and h are constants with the constraint $f > g$.

2. The proposed pre-processing stage and results

As there are no boundaries of a particular object on the images no direct geometrical (translation, rotation, size) invariant transformation could not be considered. The constraint, to take account all the pixels lying in the region of interest (ROI), was evident. A ROI size 105 x 274 pixels, was enough to contain all typical defects in the images of the welds. Each ROI was obtained by convolving a window of 105 x 274 pixels with the current image, from left to right and from top to bottom. Each window, in both x and y directions, had at least an overlapping of 25% with its neighbouring previous positions. The pixels that fell into the current window were used to calculate a slop histogram onto each axis x and y, with the goal to estimate the homogeneity of its content in term of pixel intensity. In the case of heterogeneous ROI as it can be determined by the flatness of one of the slope histogram.

2.1. Application of the discret wavelet transformation

The images presented in table 1 could not pre-processed by traditional texture filtering methods like those cited in [3], because of the diversity in terms of "granularity" and "irregularity" of the texture. At the same time, images that belong to different categories may look very similar. The experiments showed that the wavelet analysis was enough sensitive to produce the data structure that could be used for features selection. An image DWT transform gives frequency and spatial information too, it can be considered semantically as the filtering of images by combining two filters – low and high pass applied simultaneously at the same time, but separately on the rows and columns of the original image. The result was a set of four images, which are the output of low/low, low/high, high/low and high/high, row/column filters. The DWT of images leads to its decomposition in four components: the approximation, and the details in three orientations: horizontal, vertical and diagonal. The same transform may be then applied on the output of the low/low filter in the previous stage, if it is needed. The paper used the Daubechies 9 wavelets to extract spatial features from the images of welds. It can be seen in Figure 3 that the resulting sub-images look like ordinary textures.

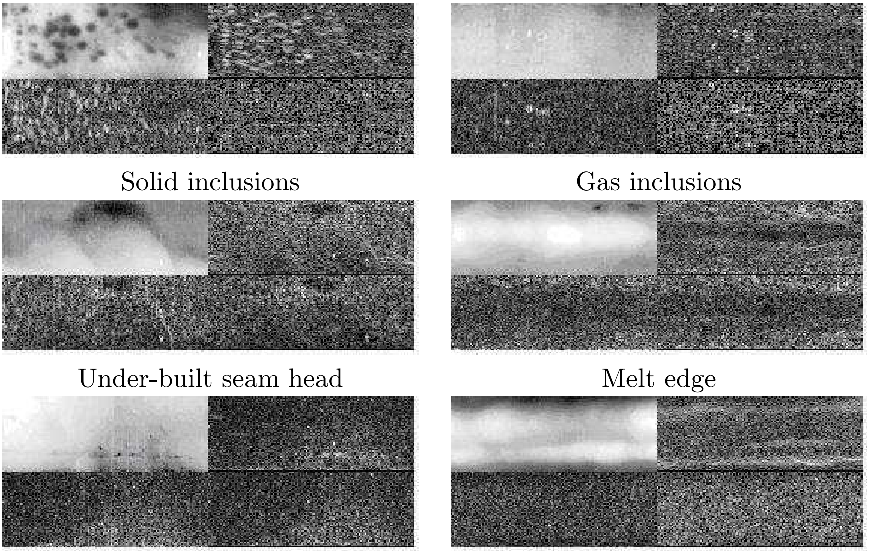

Solid inclusions | Gas inclusions

Under-built seam head | Melt edge

Under-built seam root | Under-built seam head

Figure 4

Here the aim of wavelet transformation is not to achieve a compression of images. The computed wavelet coefficients are located in four matrixes; they are not quantized but are instead saved for use as input to the ICM as it was been described above in the paper. The number of stages in wavelet decomposition that leaves the weld images distinguishable or interpretable by human eyes is two. This number can then be the natural stopping criterion for the analysis process instead of the result of an entropy calculation. In this paper only one stage is accomplished to reduce the amount of data to be processed without loosing of accuracy in the final results.

Differences between some images of different category can be very small, as can be seen in Figure 1. On the other hand the differences between ones of the same category can be significant. This is a potential problem for some methods filtering techniques based on the calculation of dot products during convolution of the filter mask with the image.

There exist a large number of wavelet families having different analysis properties. Among these properties, in this paper, the experiments show that two are of relevant importance: the regularity and the capacity of sensing high order polynomial components of the analysed signal. The first one is a structural property of the Daubechies 9 wavelets that makes them to be excellent in local regularity or irregularity extraction. On top of this, there is a fast orthogonal transform implementing its algorithm. The second property is obtained by setting the number of vanishing moments to 10. Since, initially the amount data to be processed is enough large the paper used the DWT instead of CTW which is time consuming leaving a lot of redundant output coefficients. It is important to notice that the four sets of coefficients of the SWT are considered as four complementary sides of the original image.

2.2. The modified PCNN algorithm

The PCNN/ICM models do not need training in difference of several neural networks models; hence they need a lot of parameters to be initialized. The paper used the both PCNN and ICM models without any sensible difference in results, but the ICM algorithm was twice fast. The input to the PCNN/ICM is the normalised 105 x 274 2D matrix of each subset of data (from a given sub-band filter) generated by the DWT from the original grey-scale image. The weakness of the original the PCNN algorithm is the no-existence of a general stopping criterion, in other word the number of iteration is application specific and is not yet formalised. Without a specified number of iterations the PCNN processing turns in time wasting and on top of that the feature extraction can not embed generalization and discrimination constraints needed for future categorization. Another problem that correlates with the original PCNN algorithm is the impossibility to generate geometrically invariant feature set and consistent data structure by calculating the signature of the resulting output image in each iteration, as described in [2].

This paper uses the empiric solution by examining visually the binary outputs of PCNN and registered the exact number of iterations needed for each image in a set of 150 images.

Experimental foundations of the proposed method are based on the following observations:

- The number of iterations needed for the PCNN to produce good results is image category independent variable.
- The number of iteration cannot be expressed by first-order texture statistics
- The weld images that needed the same number of iterations for processing, have nearly the same values for texture features based on the gray-level co-occurrence (GLCM).
- The mapping can be done by mean of classical regression ANN having a reasonable size.

The proposed GLCM features are:

- Contrast:

$$F0 = -\sum_i \sum_j (i-j)^2 P[i,j] \tag{2.1}$$

- Energy or Angular Second Moment:

$$F1 = \sum_i \sum_j P^2[i,j] \tag{2.2}$$

- Homogeneity:

$$F2 = \sum_i \sum_j \frac{P[i,j]}{1 + [i - j]} \tag{2.3}$$

- Correlation:

$$F3 = \sum_i \sum_j \frac{(i-\mu)(j-\mu)P[i,j]}{\sigma^2} \tag{2.4}$$

The table below shows the input GLCM features and the output of the regression ANN for the images already shown in Figure 4.

	F0	F1	F2	F3	PCNN iterations
Solid inclusions	934.7242	0.0050322	0.21307	0.82643	17
Gas inclusion	767.5	0.0059825	0.24779	0.88234	14
Melt edge	979.66	0.0011426	0.19354	0.87773	9
Under-built seam root	510.37	0.0014192	0.21113	0.94138	3
Under-built seam head	851.95	0.0023694	0.21393	0.86839	6
Over-built seam head	923.92	0.0019568	0.18794	0.80033	21

Table 1

Figure 5 shows the processed images as indicated by the output of the regression ANN.

The modifications added into the original PCNN as resumed as following:

- An iteration memory trained by regression ANN is added.
- Two counters are added to the PCNN architecture. The first C1 stores the actual and effective number of iterations; the second C2 is the maximum number of iterations obtained during training the iteration memory. When C2 is enabled, the PCNN grid can be used for image signature generation and there is problem with missing values in the signature vectors because all have the same length, so the input data structure for a further classifier is consistent.
- A perceptive "curtain" is added that is enabled when C1 reaches the zero value.

A relevant parameter setting in the PCNN grid is the initialization synaptic weights matrices M and W. Here the connection mode is given by a 5×5 kernel matrix K which is Gaussian type. The central element of K matrix is 1 and the others are generated by evaluation of the Euclidian distance between two neurons. The PCNN kernels are important because their type affects the auto-wave in the grid.

All computational experiments were done in the Matlab software environment using the signal processing, image processing and neural networks toolboxes.

Solid inclusions

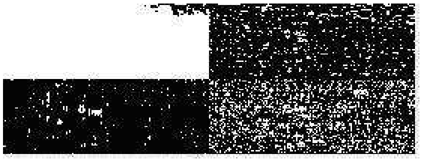

Gas inclusions

Under-built seam head

Melt edge

Under-built seam root

Under-built seam head

Figure 5

3. Conclusions

The experiments show that the wavelet transform as image multi-resolution feature extraction tool on top of a spiking neural network in occurrence the modified PCNN model can extract features that meet two important criterions: generalisation and discrimination. These goals are not satisfied when using classical filtering methods based on dot products calculation.

The modified PCNN architecture uses variable iteration numbers, to improve immunity against noises caused by over or under processing.

The proposed pre-processing produces more deterministic results that embed discriminatory and generalisation properties in the feature vectors.

The extended PCNN also can produce a geometrical invariant feature sets compared to known classical pre-processing approaches.

Further study can be done to formalise the stopping criterion.

References

[1] Izhikevich, E. M., Which Model to Use for Cortical Spiking Neurons?, *IEEE transactions on neural networks*, vol. 15, No 5, (September 2004).

[2] Linblad, T., Kinser, J. M., Image Processing Using Pulse-Coupled Neural Networks, *Springer-Verlag,* Berlin, (2005).

[3] Pun, C.-M., Rotation-invariant texture feature for image retrieval, *Computer Vision and Image Understanding,* (2003), 24–43.

[4] Pitas, I., Kouropoulos, C., Nonlinear Model-Based Image/Video Processing and Analysis, *John Wiley & Sons*, (2001), 269-307.